A FEM-MPM Hybrid Coupled Framework Based on Local Shear Strength Method for Simulating Rainfall/runoff-induced Landslide Runout

Yulong Zhu[1], Tatsuya Ishikawa[2*], Yafen Zhang[3], Binh T. Nguyen[4], and Srikrishnan Siva Subramanian[5]

[1] School of Water Resources and Hydropower Engineering, North China Electric Power University, Changping Beinong 2#, Beijing, China.

Email: zhuyulong@ncepu.edu.cn

[2*] Laboratory of Analytical Geomechanics, Faculty of Engineering, Hokkaido University, Kita 13, Nishi 8, Kita-ku, Sapporo, Hokkaido 060-8628, Japan. (Corresponding author)

Email: t-ishika@eng.hokudai.ac.jp

[3] School of Engineering, The Open University of China, Haidian Wukesong, Beijing, China.

Email: zhangyafen@ouchn.edu.cn

[4] Research and Development Center, Nippon Koei Co., Ltd, 2304 Inarihara, Tsukuba, Ibaraki 300-1259, Japan.

Email: nguyen-binh@frontier.hokudai.ac.jp

[5] State Key Laboratory of Geo-hazard Prevention and Geo-environment Protection, Chengdu University of Technology, Chengdu, China.

Email: srikrishnan@frontier.hokudai.ac.jp

Highlights

1. A local shear strength method is proposed for evaluating the variation of the shear strength for each soil material point.
2. A FEM-MPM hybrid coupled framework is proposed to simulate rainfall/runoff triggered landslide runout in unsaturated slopes.
3. Simultaneous analysis of runoff, seepage, and landslide runout within a small catchment scale is successfully performed.

Abstract

Limited by the independence and its defects of each general software package, simultaneous analysis of runoff, seepage, and large-deformation analysis is still an inevitable challenge. Generally, one of seepage, landslide-related large-deformation, and runoff is ignored or indirectly assessed during unsaturated soil landslide runout simulation. To provide a brand new solution, this paper declares a local shear strength (LSS) method to evaluate rainfall/runoff-induced reduction of the unsaturated soil shear strength. After that, a hybrid coupled hydro-mechanical framework is proposed to simulate rainfall/runoff-induced landslide runout within an unsaturated soil slope. The decrease in local shear strength corresponding to the decrease in matric suction is defined by shifting the Mohr-Coulomb (M-C) failure envelope towards compressive stress space during rainfall/runoff infiltration. Based on the proposed local shear strength method, the variable matric suction obtained from the bidirectionally coupled runoff and seepage analysis in FEM is unidirectionally transferred to the variable local shear strength for each soil material point in MPM (i.e., this is a FEM-MPM hybrid coupled model). Then, the correctness of the proposed hybrid coupled hydro-mechanical framework is effectively verified by a hypothetical homogeneous slope model. The results show that the slope stable/unstable state simulated by the proposed hybrid coupled hydro-mechanical framework has a good consistency with that simulated by the shear strength reduction technique (SSRT) and limit-equilibrium method (LEM). Afterward, combined with a case study of a natural landslide in Hokkaido, Japan, it is proved to be effective for simulating landslide runout subjected to rainfall/runoff infiltration by using the proposed hybrid coupled hydro-mechanical framework in an unsaturated soil slope.

***Keywords*:** Local shear strength method; Material point method; Rainfall/runoff-induced landslide runout; Finite element method; Unsaturated soil slope

1. Introduction

In many mountainous regions, rainfall/runoff is considered to be the main cause triggering landslides/slope failures. With the intensification of global and regional climate change, extreme rainfall events and huge flooding have occurred frequently in recent years (Paerl et al., 2020; Wei et al., 2020). The decrease in matric suction in the unsaturated zone caused by rainwater infiltration under torrential rain is considered the main cause of the landslide/slope failure initiation (Zhu et al., 2020). After the landslide/slope failure occurs, the collapsed soil moves downward, namely landslide runout, threatening the lives and properties of residents living downslope, especially those living near the foothills. Therefore, it is of great social and economic value to study the landslide runout distance, reasonably install the disaster prevention measures, and set the evacuation area. Many scholars have made great efforts to develop numerical methods for simulating landslide runout, e.g. Discrete Element Method (DEM) (An et al., 2021), Discontinuous Deformation Analysis (DDA) (Shi, 1989; Peng et al., 2020), and Material Point Method (MPM) concurrently researched and operated by several groups (Müller and Vargas, 2019; Acosta et al., 2021; Sun et al., 2021; Ying et al., 2021). Among them, DEM and DDA consider the geo-material as discrete blocks connected by spring units. Though DEM and DDA are recognized as having the advantages to simulate the cracking behaviors of continuous media or model the contact, collision, slipping, and movement of discretely stacked materials, these two methods also suffer from low convergence, low accuracy, high calibration

requirements, and high computational costs. Besides, runoff and seepage analysis are still considered as the main limitations of them. Furthermore, a depth-integrated continuum method that uses continuum to model landslide mobility is recently developed by Iverson et al. (2015), Ouyang et al. (2017), and Ouyang et al. (2019). In this method, integrated by the Navier-Stokes equations and flow depth, the mass and momentum equations are solved by using the finite difference method. Apart from these, another method, MPM, is also getting continued attention since it was first formulated by Sulsky et al. (1994), as it avoids the problem of mesh distortion problems in the FEM and shows higher computing efficiency compared with DEM and DDA. In MPM, the material bodies are represented by a large number of material points. The physical information (velocity, acceleration, mass, etc.) is stored in those material points. During the computational process of MPM, the physical information will be repeatedly converted between the background grid and the material points to form a link between the physical information and the spatial position.

The single-phase (solid phase) MPM has been maturely adopted to simulate landslides without considering hydrology. For example, Sun et al. (2015) validated the applicability of the MPM in simulating runout according to the comparative results of experiments and simulations of a simple landslide example. Woo and Rodrigo (2018) presented a generalized interpolation MPM to get higher computational accuracy and efficiency of MPM. Recently, MPM has also been developed to capture the rapid landslide behavior in the form of a soil-water mixture. The porous solid phase, pore water phase, and/or pore air phase are characterized by using two or more Lagrangian layers, i.e., two-phase MPM or multi-phase MPM (e.g., Soga et al., 2016; Liang et al., 2020; Lei et al., 2021). However, it is worth noting that the objects of the above researches are mainly rainfall-induced landslides/slope

93 failures in saturated soil or unsaturated soil. The runoff analysis with changes in water depth is
94 neglected since it is considered as one of the fundamental challenges when using either single-phase
95 and two-phase MPM or multi-phase MPM. From the view of the coupling process of runoff and
96 seepage, and the variation of matric suction in unsaturated soil, the traditional numerical method,
97 FEM, has more advantages than other methods. Further, it has been widely used in general
98 commercial software packages, which are designed to analyze runoff and seepage. For example,
99 COMSOL Multiphysics (COMSOL Multiphysics, 2018) and GEO-SEEP/W (GeoStudio International,
100 2007). Therefore, proposing a FEM-MPM coupled computational framework will give full play to
101 their respective advantages in the coupled simulation of runoff, seepage, and landslide runout.
102 Consequently, the objective of this study was to establish a coupled hydro-mechanical framework
103 to simulate landslide runout triggered by rainfall/runoff infiltration within an unsaturated slope. To
104 achieve this goal, this study firstly proposes a local shear strength method for defining the variation of
105 the local shear strength induced by the rainfall/runoff infiltration for each soil material point. Then,
106 based on the proposed local shear strength method, a hybrid coupled hydro-mechanical framework is
107 developed. In the hybrid coupled hydro-mechanical framework, the seepage behavior is captured by
108 bidirectionally coupled runoff and seepage analysis with the FEM. Then, the variable matric suction
109 obtained from FEM is unidirectionally transferred to the variable local shear strength of each soil
110 material point in MPM by using the local shear strength method. The resulting slope failure behavior
111 is analyzed by the MPM. Thus, a FEM-MPM hybrid coupled model is established. Finally, through a
112 validation model and a case study of a natural slope, the results proved that the proposed FEM-MPM

hybrid coupled model is effective for coupled simulating runoff, seepage, and large-deformation problems, such as rainfall/runoff-induced landslide runout within an unsaturated slope.

2. Definition of local shear strength for each unsaturated soil material point

The saturated soil shear strength for each material point is defined by the Mohr-Coulomb (M-C) failure criterion,

$$\tau_f = c' + \sigma' \tan \phi' \tag{1}$$

where, τ_f is the shear strength (kPa); c' is the effective cohesion (kPa); ϕ' is the effective internal friction angle (°); σ' is the effective normal stress on failure plane (kPa).

In reality, the soil above the phreatic surface is in an unsaturated state. In this state, the soil will have higher shear strength than in a saturated state. Currently, the well-known method is to describe the unsaturated soil behavior by using Bishop's effective stress concept (Bishop, 1959),

$$\sigma' = (\sigma - u_a)_f + \chi(u_a - u_w)_f \ , \ \chi = \frac{S_e - S_r}{1 - S_r} \tag{2}$$

where, u_a is pore air pressure (kPa), u_w is pore water pressure (kPa); σ is total normal stress (kPa); χ is effective stress parameter; S_e is effective degree of saturation; S_r is residual degree of saturation.

The unsaturated soil shear strength is also defined by Fredlund et al. (1978),

$$\tau_f = c' + (\sigma - u_a)_f \tan \phi' + (u_a - u_w)_f \tan \phi^b \tag{3}$$

where, ϕ^b is the angle indicating the rate of increase in shear strength relative to the matric suction $(u_a\text{-}u_w)_f$.

Eqs. (2) and (3) present proper compliance with in-door test results and have been widely used (Vanapalli et al., 1996). Vanapalli et al. (1996) discussed the applicability of the above two shear strength models in geotechnical engineering practice and built the relationship between the two

models,

$$\chi = \frac{\tan \phi^b}{\tan \phi'} \tag{4}$$

Therefore, the unified equation form can be written as,

$$\tau_f = c' + (\sigma - u_a)_f \tan \phi' + (u_a - u_w)_f \chi \tan \phi' \tag{5}$$

which also can be written as,

$$\tau_f = \underbrace{\left[c' + (u_a - u_w)_f \chi \tan \phi'\right]}_{c'_f} + (\sigma - u_a)_f \tan \phi' \tag{6}$$

where, c_f' is the intercept at a specific matric suction, $(u_a - u_w)_f$, (kPa).

Conventionally, the M-C failure envelope is fixed for the entire slope during rainfall infiltration. Changes in pore water pressure caused by rainfall/runoff infiltration only affect the scaling and translation of the stress circle. Meanwhile, at present, describing the difference in matric suction induced by runoff of various material points is still a potential challenge of the MPM. Therefore, according to Eq. (6), the variation of local shear strength for each material point in MPM can be described by including matric suction in the cohesion intercept. The new cohesion intercept, c_f', is called the total cohesion intercept. This provides a feasible way to define the variation of matric suction and local shear strength for each soil material point in the unsaturated region, as cohesion is one of the material properties that must be assigned during the modeling process. Eq. (6) suggests that a decrease in local shear strength (the intercept of the M-C failure envelope decrease) corresponding to a decrease in matric suction during rainfall/runoff infiltration is defined by shifting the M-C failure envelope towards compressive stress space as illustrated in Fig. 1. Consequently, the influences of matric suction changes on the variation of the local shear strength of each soil material point in the

unsaturated region can be considered by using the proposed local shear strength method as shown in Fig. 1.

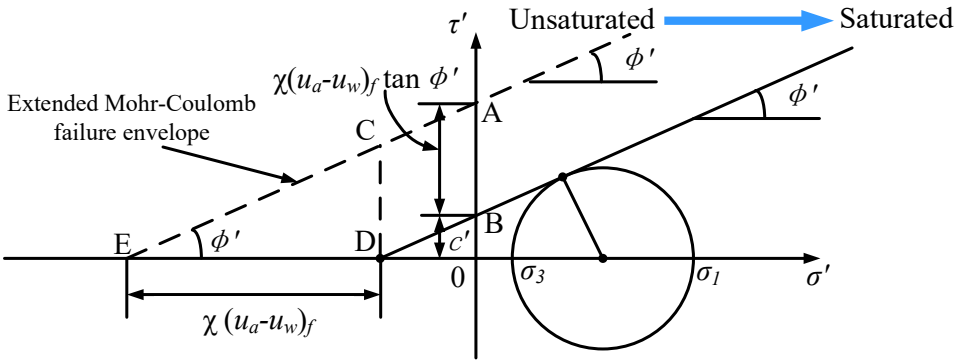

Fig. 1. Local shear strength (LSS) for each unsaturated material point.

3. Hybrid coupled hydro-mechanical framework and governing equations

Based on the proposed local shear strength method, this section firstly proposes a hybrid coupled hydro-mechanical framework of FEM and MPM to simulate runoff, seepage, and large-deformation of the unsaturated soil slope. Then, the governing equations used in the runoff model, seepage model, and soil mechanics model are presented.

3.1 Hybrid coupled hydro-mechanical framework

During a rainstorm or torrential rain, the generation of runoff has a significant impact on soil moisture, ground surface erosion, and landslides. Meanwhile, in unsaturated soils, the variation of volumetric water content affects matric suction, which thereby affects local shear strength. It also affects the self-weight and stress distribution. Therefore, the effects of runoff on the soil moisture changes, and the effects of soil moisture changes on local shear strength and self-weight of unsaturated soil are considered in the coupled hydro-mechanical framework. In the hybrid coupled hydro-mechanical framework, the runoff and seepage are simulated by using the PDEs (partial differential equations) module in the FEM software, COMSOL Multiphysics (COMSOL Multiphysics,

172 2018), while the large-deformation of the landslide is simulated by using MPM3D (an MPM code that
173 was programmed by the group led by Prof. Zhang Xiong at Tsinghua University,
174 http://comdyn.hy.tsinghua.edu.cn/english/mpm3d). The coupled hydro-mechanical framework is
175 shown in Fig. 2. The runoff model and seepage model in FEM are bidirectionally coupled through the
176 interaction between surface water and groundwater (infiltration and exfiltration). The water depth
177 calculated from the runoff model is applied to the seepage model as the water head boundary
178 condition. The inflow velocity (infiltration) and outflow velocity (exfiltration) calculated from the
179 seepage model is returned to the runoff model as the source of water. The coupling process is
180 described in detail elsewhere (Zhu et al., 2020). The FEM analysis and MPM analysis are
181 unidirectionally coupled in two means: (1) the influence of changes in soil moisture content (FEM
182 output) on self-weight (MPM input) is taken into account in the elastoplastic model, and (2) the
183 influence of matric suction (FEM output) on the local shear strength (MPM input) is considered by
184 using the local shear strength method. It is worth noting that as shown in Fig. 2, the proposed
185 FEM-MPM coupled model is not a fully coupled model but a hybrid coupled model. Runoff and
186 seepage analysis is bidirectionally coupled through infiltration and exfiltration in the FEM analysis,
187 while the FEM analysis provides inputs to the MPM analysis, meaning that this process is
188 unidirectionally coupled. Furthermore, under the proposed framework, during the long-term coupled
189 runoff and seepage analysis, it is assumed that the deformation of the slope is not considered because
190 the slope is remaining stable at this time. While during the large-deformation analysis when the
191 landslide occurs, the change of seepage force, shear strength, and pore water pressure are neglected as

slope failure is a quickly triggered and rapidly developing geological hazard. Therefore, these assumptions are the limitations of the proposed coupled hydro-mechanical framework.

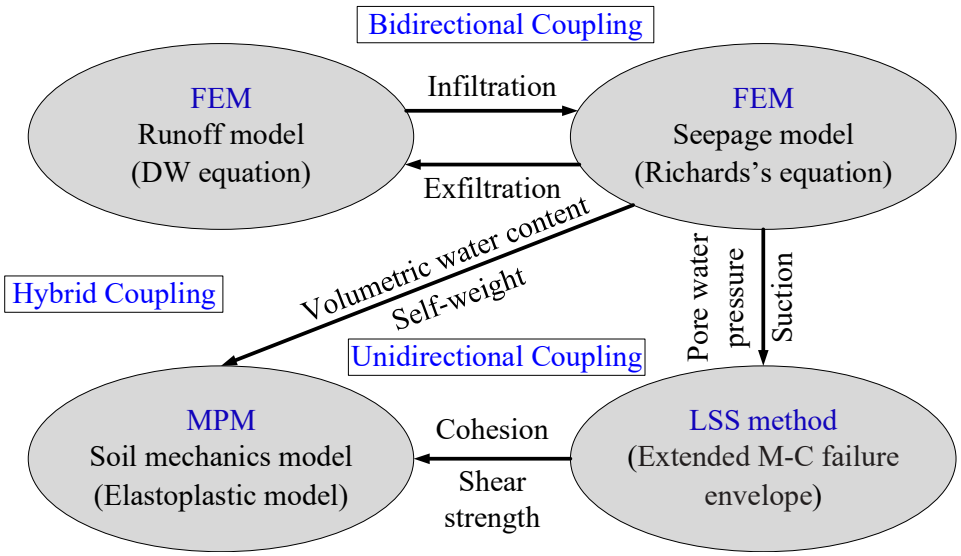

Fig. 2. Hybrid coupled hydro-mechanical framework of FEM and MPM.

3.2 Governing equation for runoff analysis

Runoff analysis is governed by the diffusion wave (DW) equation as shown in Eq. (7) (Weill et al., 2009; Zhu et al., 2020),

$$\frac{\partial h}{\partial t} - \nabla\left(\frac{h^{5/3}}{n_m\sqrt{|S|}}\nabla(H)\right) = R - I \tag{7}$$

where, I is infiltration/exfiltration rate (m/s); t is time (s); n_m is Manning's roughness coefficient (s/m$^{1/3}$); h is runoff depth (m); H is water surface elevation (m); R is rainfall intensity (m/s); S is water surface gradient, which can be replaced by slope gradient due to the small difference between them (Weill et al., 2009).

3.3 Governing equation for seepage analysis

Seepage analysis is governed by the equation proposed by Richards (1931) which can be expressed as follows,

$$\nabla \cdot \left[k_s\, k_r \cdot \nabla\left(H_p + z\right)\right] + Q_w = \left[C_m + S_e S_c\right]\frac{\partial H_p}{\partial t} \tag{8}$$

where, Q_w is sink and source of water (s^{-1}), which is related to I; k_s is saturated hydraulic conductivity (m/s); C_m is specific moisture capacity (m^{-1}); k_r is relative hydraulic conductivity; S_c is specific storage coefficient (m^{-1}); H_p is pressure head (m); S_e is the effective degree of saturation; z is the elevation (m). The relationship in C_m, S_e, k_r, θ, and H_p in unsaturated soil can be calculated by θ_s, θ_r, and the vG parameters, *a, n, m,* and *l* (van Genuchten, 1980).

$$\theta = \theta_r + S_e(\theta_s - \theta_r) \tag{9}$$

$$S_e = \frac{1}{\left[1+(aH_p)^n\right]^m} \ , \ m = 1 - \frac{1}{n} \tag{10}$$

$$C_m = \frac{am}{1-m}(\theta_s - \theta_r)S_e^{\frac{1}{m}}(1 - S_e^{\frac{1}{m}})^m \tag{11}$$

$$k_r = S_e{}^l \left[1 - (1 - S_e^{\frac{1}{m}})^m\right]^2 \tag{12}$$

3.4 Governing equations in MPM

In MPM. each computational step can be divided into three phases: initial phase, Lagrangian phase, and convective phase as shown in Fig. 3 (Sun et al., 2015). In the initial phase, the physical information stored in material points (e.g., locations, velocities, mass, etc.) is mapped on the Lagrangian background grid to get the initial solution values. In the Lagrangian phase, the material points move with the Lagrangian background grid and the global equations are solved within the Lagrangian background grid. After that, the stored physical information is updated. In the convective phase, the Lagrangian background grid is reset, while the stored physical information remains unchanged.

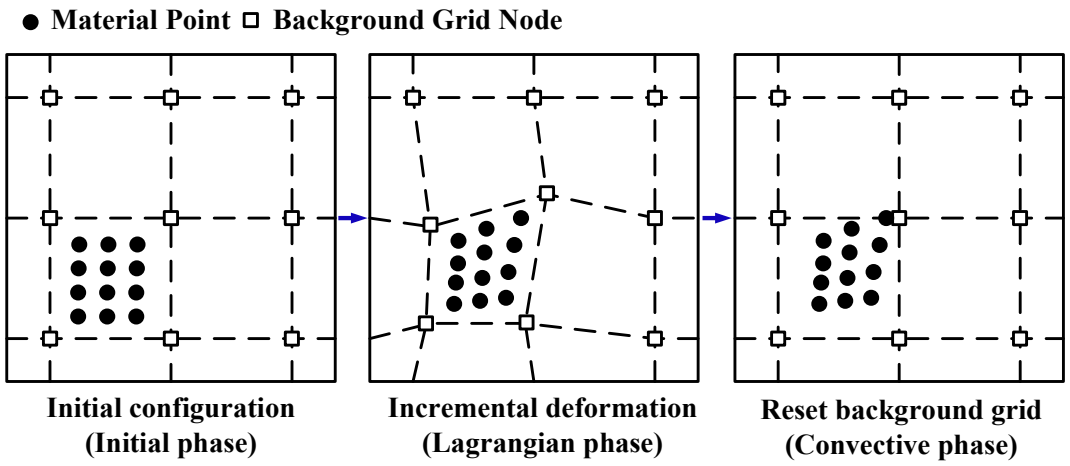

Fig. 3. Three phases of one computational step of MPM (adapted from Sun et al. (2015)).

The governing equations of large-deformation analysis in MPM can be expressed as follows (Abe et al., 2013):

$$\frac{d\rho(\theta)}{dt} + \rho(\theta)\nabla \cdot \boldsymbol{v} = 0 \quad \text{(Conservation of mass)} \tag{13}$$

$$\rho(\theta)\boldsymbol{a} = \nabla \cdot \boldsymbol{\sigma} + \rho(\theta)\boldsymbol{b} \quad \text{(Conservation of momentum)} \tag{14}$$

where, $\rho(\theta)$ is soil-water mixture density (kg/m^3) as a function of volumetric water content (θ); $\boldsymbol{a}$ is acceleration vector (m/s^2); $\boldsymbol{v}$ is velocity vector; $\boldsymbol{b}$ is body forces vector (m/s^2); $\boldsymbol{\sigma}$ is stress tensor (kPa) (m/s).

4. Validation of the proposed hybrid coupled hydro-mechanical framework

To check the reliability of the hybrid coupled hydro-mechanical framework proposed in this study for simulating unsaturated soil slope instability, a validation model is simulated by the FEM-MPM hybrid coupled model compared with the other two commonly used methods: limit-equilibrium method and shear strength reduction technique. In the validation model, the water supply (rainfall and runoff) is not considered. The two side walls and bottom are impermeable to water. The groundwater level (GWL) is assumed to be -5 m. Table 1 lists the soil properties used in the validation model. The model size and boundary conditions are displayed in Fig. 4. The simulation results of the shear

strength reduction technique are obtained from COMSOL, and the simulation results of the limit-equilibrium method are obtained from another commercial slope-stability software package GEO-SLOPE/W (GeoStudio International, 2007).

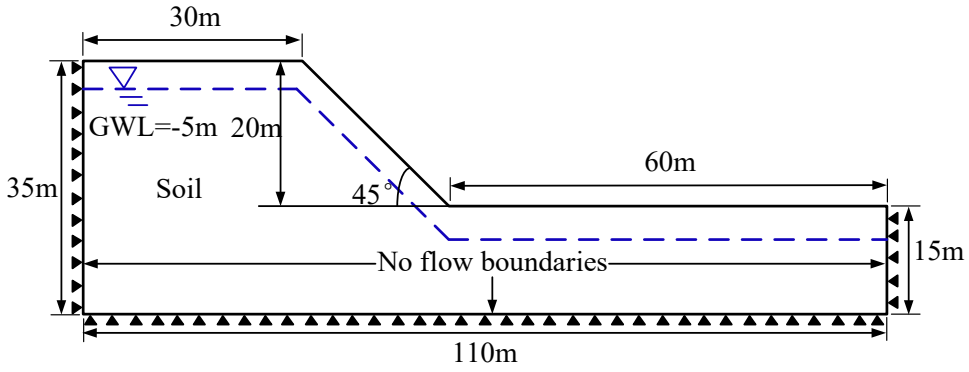

Fig. 4. Schematic diagram of the validation model.

The comparison of the simulation results calculated by shear strength reduction technique, limit-equilibrium method, and the proposed FEM-MPM hybrid coupled model are shown in Fig. 5. Fig. 5(a) shows the slope in the stable state. Fig. 5(b) shows the slope in the critical state. Fig. 5(c) shows the slope in the failure state. In each sub-figure (Fig. 5(a), Fig. 5(b), and Fig. 5(c)), Fig. 5(I) displays the pressure head calculated by FEM. Fig. 5(II) displays the slip surface simulated by limit-equilibrium method with the factor of safety (FOS). Fig. 5(III) displays the results simulated by the shear strength reduction technique. Fig. 5(IV) displays the ultimate slope failure shape simulated by the proposed FEM-MPM hybrid coupled model. From Fig. 5(a), it is recognized that the slope simulated by the proposed FEM-MPM hybrid coupled model is stable. The FOS calculated by the limit-equilibrium method (FOS=1.198) in Fig. 5(a)(II) and that calculated by the shear strength reduction technique (FOS=1.190) in Fig. 5(a)(III) are larger than 1.0. From Fig. 5(b), it is recognized that the slope simulated by the proposed FEM-MPM hybrid coupled model is in a critical state. At the same time, the FOS calculated by limit-equilibrium method (FOS=0.996) in Fig. 5(b)(II) and that

calculated by shear strength reduction technique (FOS=0.930) in Fig. 5(b)(III) are slightly less than 1.0, meaning that the slope is unstable under the pore water pressure distribution at this time. From Fig. 5(c), it is recognized that the slope simulated by the proposed FEM-MPM hybrid coupled model is failed. The FOS calculated by the limit-equilibrium method (FOS=0.567) in Fig. 5(c)(II) and that calculated by shear strength reduction technique (FOS=0.590) in Fig. 5(c)(III) are much less than 1.0. From Fig. 5(a), Fig. 5(b), and Fig. 5(c), it indicates that the slope stable/unstable state simulated by the proposed FEM-MPM hybrid coupled model is consistent with that calculated by the limit-equilibrium method and the shear strength reduction technique. The similar slip surface shapes and stable/unstable state calculated by the proposed FEM-MPM hybrid coupled model, limit-equilibrium method, and shear strength reduction technique give a good verification of the proposed FEM-MPM hybrid coupled model on simulating slope instability in unsaturated soil, although the slip surface calculated by shear strength reduction technique is slightly shallower in Fig. 5(b) and Fig. 5(c). The main reason could be that the slip surface calculated by the shear strength reduction technique is the initial slip surface. Due to the calculation of the shear strength reduction technique is terminated due to non-convergence after the shallow layer is damaged, the development process of the slip surface from the initial stage to the ultimate stage is not considered by the shear strength reduction technique.

Table 1 Soil properties used in the validation model.

Dry density, ρ_s (kg/m^3)	Effective cohesion, c' (kPa)	Effective internal friction angle, ϕ' (°)	Young's modulus, E (MPa)	Poisson's ratio, v
1695	0 and 10	20 and 30	50	0.3
Saturated hydraulic conductivity, k_s (m/s)	Saturated vol. water content, θ_s (m^3/m^3)	Residual vol. water content, θ_r (m^3/m^3)	vG parameter, α	vG parameter, m

			(1/m)	
1.12×10^{-5}	0.36	0.035	0.538	0.468

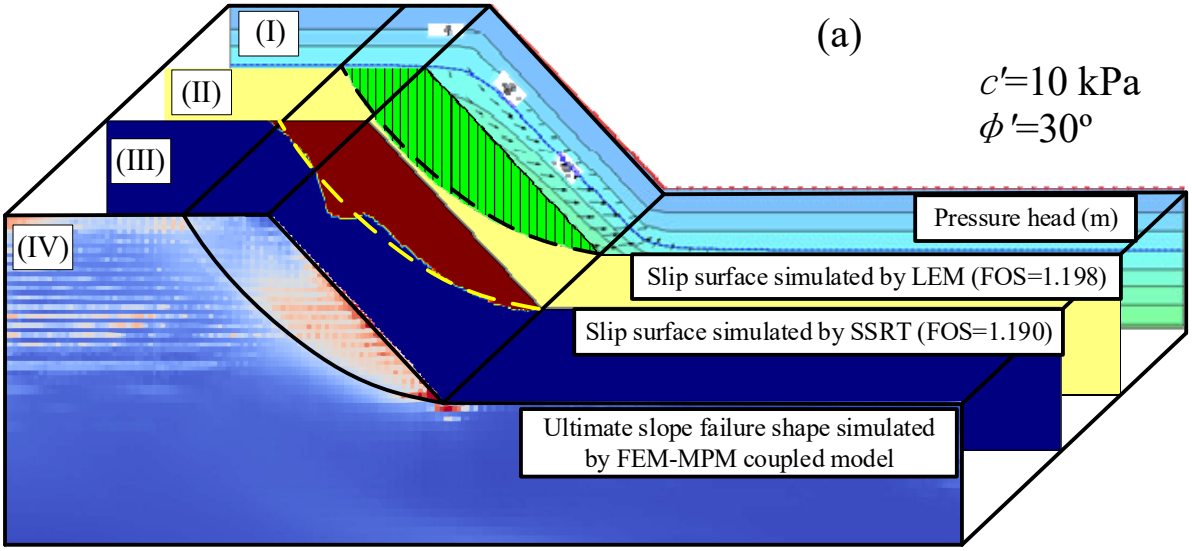

279

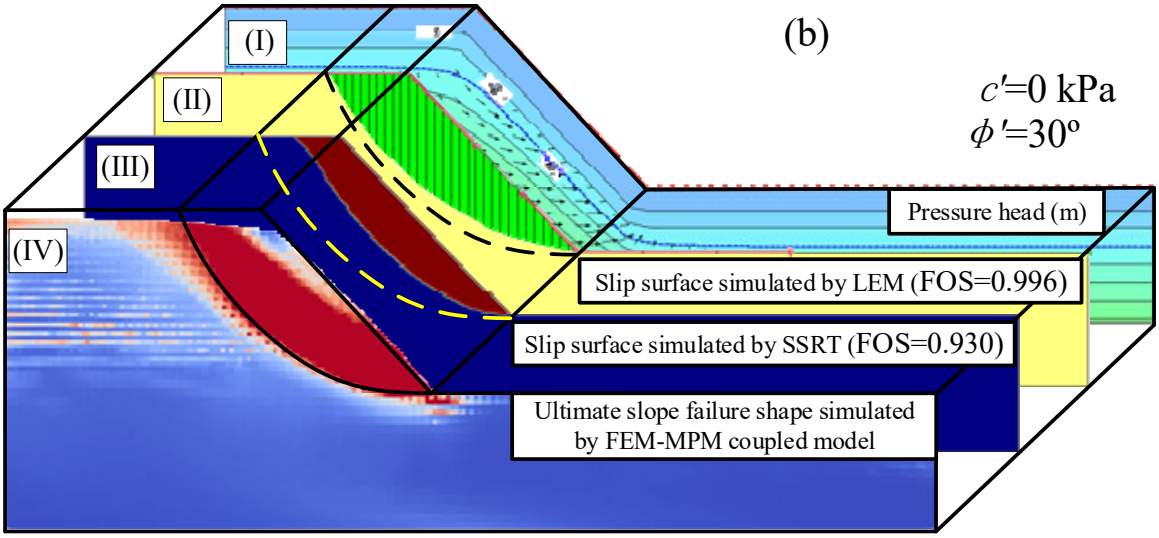

280

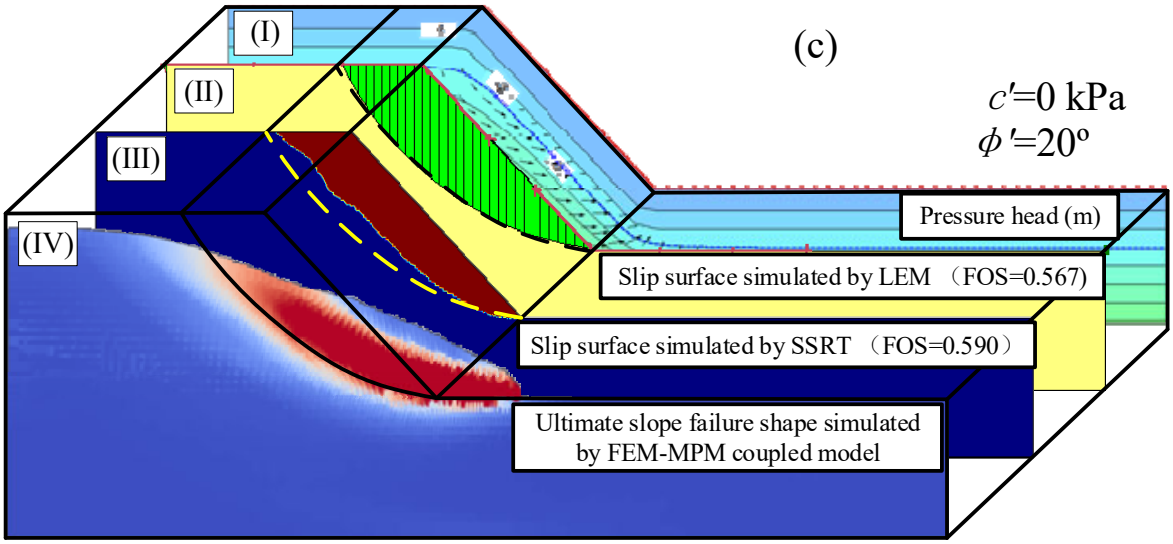

281

282 **Fig. 5.** Numerical results calculated from limit-equilibrium method, shear strength reduction

283 technique, and FEM-MPM hybrid coupled model. (a) Stable state; (b) Critical state; (c) Failure state.

284 In each sub-figure, (I) pressure head calculated by FEM, (II) slip surface with FOS simulated by

285 limit-equilibrium method, (III) slip surface with FOS simulated by shear strength reduction technique;

286 (IV) ultimate slope failure shape simulated by FEM-MPM hybrid coupled model.

287 ## 5. Natural landslide simulation by the proposed FEM-MPM hybrid coupled model

288 ### 5.1 Numerical model and soil properties

289 In 2016, typhoon No.10 hit Northern Japan at the end of August. During this period, several

290 serious landslides occurred, for example, at location 1 in Fig. 6. The landslide is located in the Hidaka

291 mountains in Hokkaido, Japan. The maximum observed cumulative rainfall in three days (29^{th}-31^{st})

292 reached 488 mm as plotted in Fig. 7. The geological conditions of this site are dominated by

293 metamorphic rocks and plutonic rocks that belong to the Hidaka metamorphic belt. It is mainly

294 composed of medium-grained and massive granite containing biotite. The shallow part of the granite

295 that penetrates the sedimentary rocks of the Hidaka metamorphic belt is being weathered, forming a

layer of weathered residual soil about 10 m on the ground surface. Focus on the target area surrounded by the red dashed rectangle in Fig. 6, a three-dimensional (3D) model for runoff and seepage analysis was built as displayed in Fig. 8(a). Fig. 8(b) displays the cross-section at Location 1. Only one two-dimensional (2D) profile at Location 1 was simulated by the MPM model for large-deformation analysis. Fig. 8(c) displays the material points with the number of 10,487 within the 2D profile. More simulations of 2D profiles along the sliding direction are repetitive work, so they are not carried out in this study.

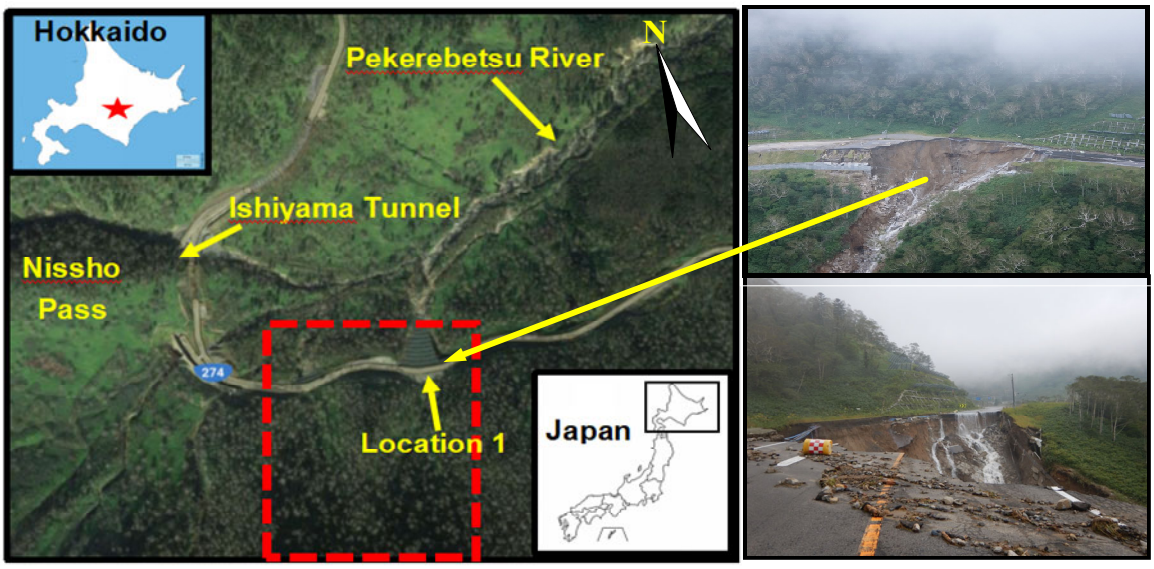

Fig. 6. Locations and performance of slope failure.

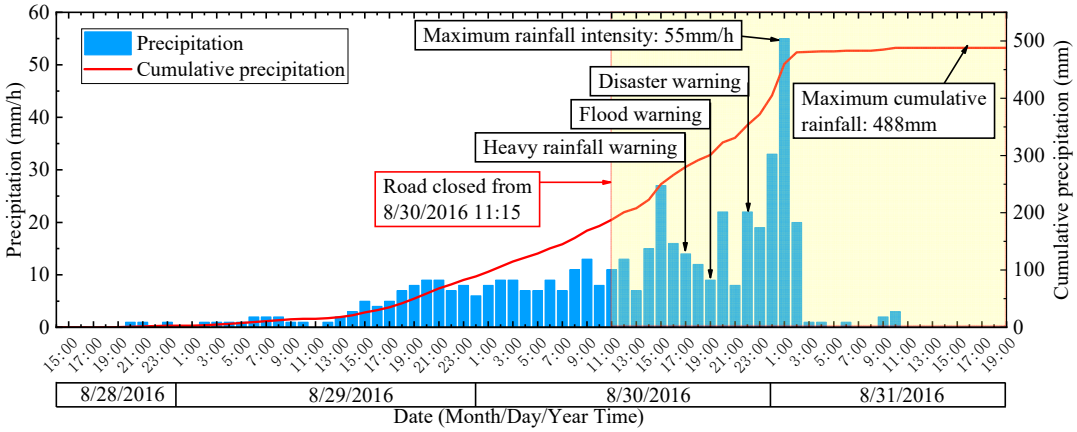

Fig. 7. Recorded rainfall during typhoon No.10.

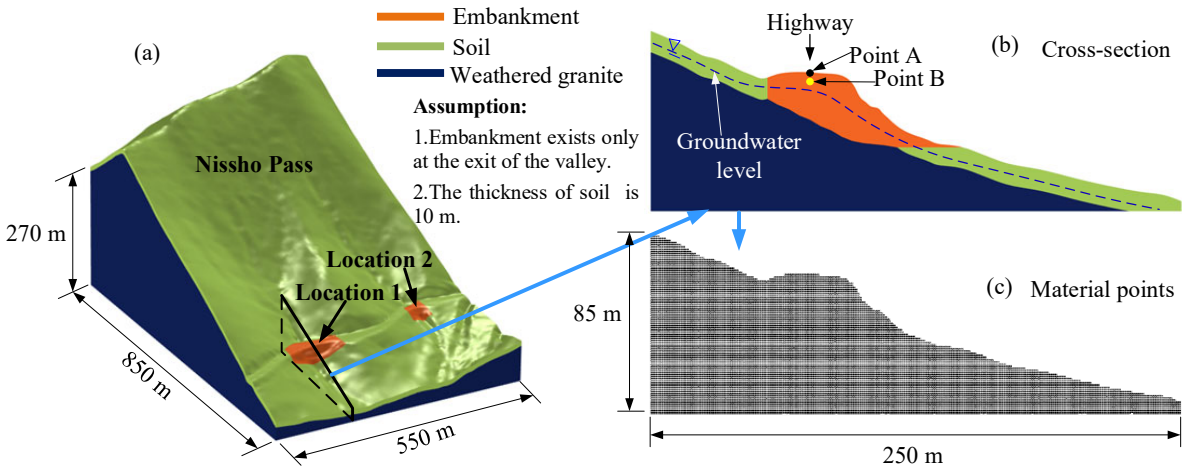

307

308 **Fig. 8**. (a) 3D numerical model of the target area; (b) Cross-section at Location 1; (c) Material

309 points at Location 1.

310 In the 3D model, the geological composition information is shown in Fig. 8(a), and it is

311 considered that the embankment exists only at the exit of the valley and the thickness of the soil is 10

312 m. Soil properties are listed in Table 2. The parameters i.e. dry density (ρ_s), saturated hydraulic

313 conductivity (k_s), saturated volumetric water content (θ_s), effective cohesion (c'), and effective friction

314 angle (ϕ'), Young's modulus (E), and Poisson's ratio (v) have been obtained from laboratory element

315 tests (Sato et al., 2017). The parameters for which no results of laboratory tests are available, i.e.,

316 residual volumetric water content (θ_r) and van Genuchten parameters (α and m) were estimated based

317 on the grain size curve of soil by using the software, SoilVision (SoilVision, 2018). SoilVision is

318 geotechnical database software that contains data on over 6,200 soil samples. It can be used to

319 estimate the missing characteristic values of the soil based on the grain size curve of the soil. The

320 initial GWL is set to -5.5 m considering historical measurements. According to the value for mountain

321 grassland recommended by the Japan Institute of Country-ology and Engineering (JICE), Manning's

322 coefficient value is set to 0.3 s/m$^{1/3}$.

323 **Table 2** Soil properties used for the FEM-MPM hybrid coupled simulation.

Parameters	Dry density, ρ_s (kg/m^3)	Effective cohesion, c' (kPa)	Effective internal friction angle, ϕ' (°)	Young's modulus, E (MPa)	Poisson's ratio, v
Embankment	1695	0	37	50	0.3
Soil	1020	0	35	50	0.3
Weathered granite	2000	37	21	500	0.3
Parameters	Saturated hydraulic conductivity, k_s (m/s)	Saturated volumetric water content, θ_s (m^3/m^3)	Residual volumetric water content, θ_r (m^3/m^3)	vG parameter, α (1/m)	vG parameter, m
Embankment	1.12×10^{-5}	0.36	0.035	0.538	0.468
Soil	1.40×10^{-6}	0.63	0.190	0.810	0.012
Weathered granite	3.47×10^{-9}	0.48	0.008	0.437	0.246

324 5.2 Simulation results of the natural landslide induced by runoff

325 The bidirectionally coupled runoff and seepage analysis are firstly done with FEM. The
326 simulation time (represented by T) is a total of 70 hours from 2016-08-28 20:00 to 2016-08-31 18:00.
327 The calculation step is set as an adaptive time-stepping scheme that means the COMSOL will
328 automatically adjust the calculation time in each step to meet the desired Relative Tolerance (0.001 in
329 this study). The results output time step is 1.0 hour. That is after every hour of the bidirectionally
330 coupled runoff and seepage analysis, the volumetric water content and matric suction obtained from
331 FEM analysis are transferred to the MPM model and used for updating the information of mass
332 self-weight and local shear strength stored in each soil material point. From trial simulations, it is
333 found that from 15 s after the start of the MPM analysis, the slope failure shape does not change
334 significantly even if the calculation time is greatly increased. Therefore, the total time (represented by
335 t) for a landslide runout simulation by MPM is set to 15 s and the calculation step is 0.2 s. Fig. 9
336 shows the distribution of time-dependent water depth in the target area. In Fig. 9, it can be identified

that the overland water from the watershed is gathered at Location 1 since Location 1 is located at the exit of the valley. The water depth exceeds 0.2 m in the upstream area of Location 1, which is much larger than other parts of the highway. This was considered as the main cause of the landslide that occurred at Location 1.

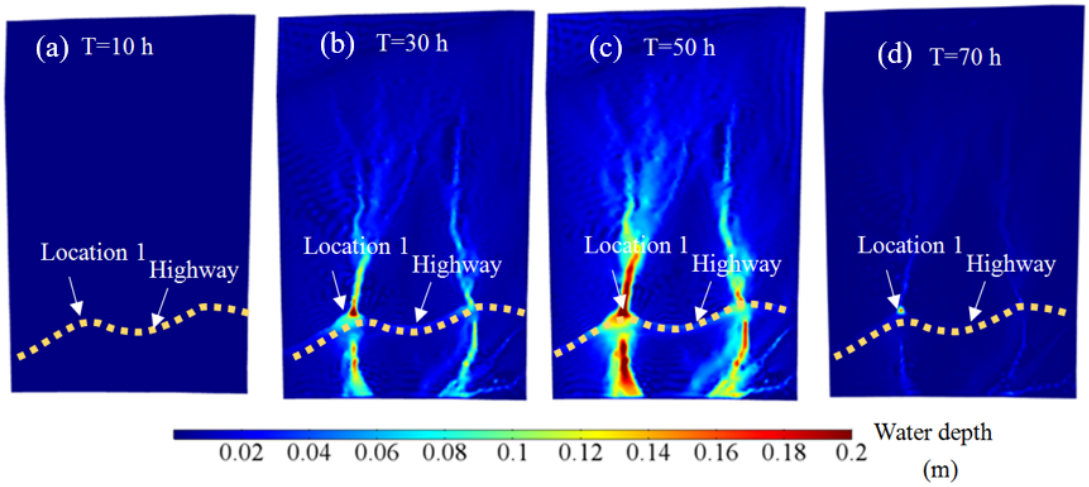

Fig. 9. Time-dependent water depth distribution at Nissho Pass (a) at T=10 h; (b) at T=30 h; (c) at T=50 h; (d) at T=70 h.

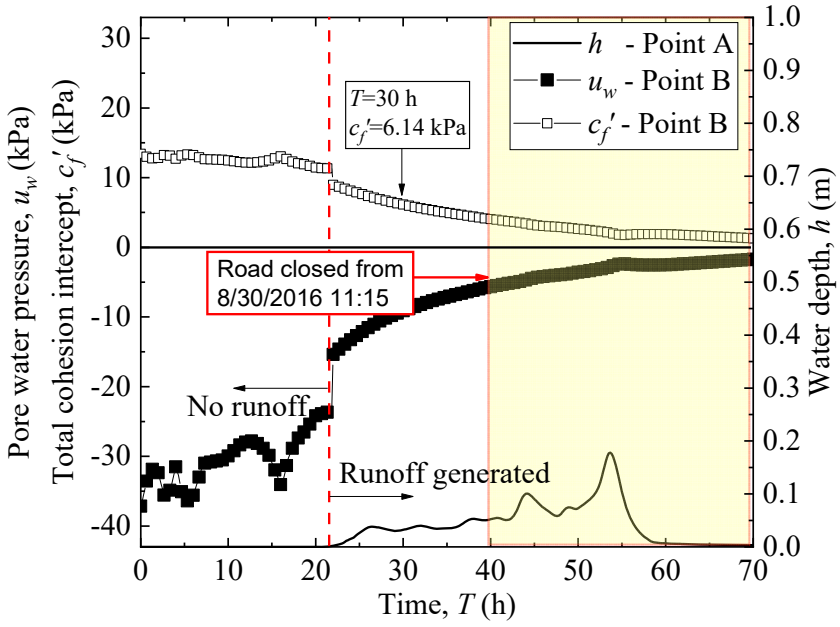

Fig. 10. Time-dependent water depth (h), pore water pressure (u_w), and total cohesion intercept (c_f').

346 The simulated water depth (h) at the road center (Point A in Fig. 8(b), located on the road
347 surface), pore water pressure (u_w), and total cohesion intercept (c_f') at an exploratory point (Point B in
348 Fig. 8(b), located at 1.0 m deep below the road surface) are plotted in Fig. 10. From Fig. 9 and Fig. 10,
349 it is identified that the generation of runoff is at 22 hours after the bidirectionally coupled runoff and
350 seepage analysis starts. After runoff is generated, there is a dramatic increase in u_w and a sudden drop
351 of c_f', meaning that the generation of runoff has a remarkable influence on the matric suction and
352 local shear strength of the embankment. Afterward, the matric suction gradually decreases to close to
353 zero, i.e., the pore water pressure (u_w) gradually increases to close to zero (soil is nearly saturated),
354 causing a continuous decrease in total cohesion intercept (c_f') of the embankment. The decrease in the
355 total cohesion intercept (c_f') leads to the decrease in the local shear strength, which causes the
356 occurrence of the landslide. Fig. 11 shows the effective degree of saturation (Se) at different times. It
357 is recognized that the unsaturated soil lies above the saturated zone. The infiltration of rainwater
358 gradually saturates the soil on the surface layer, thus resulting in the size of the unsaturated zone
359 becoming smaller. It is also identified that after runoff is generated at T=22 h, the soil on the surface
360 layer becomes saturated at T=30 h in Fig. 11 and the saturated area gradually increases with time after
361 T=30 h.

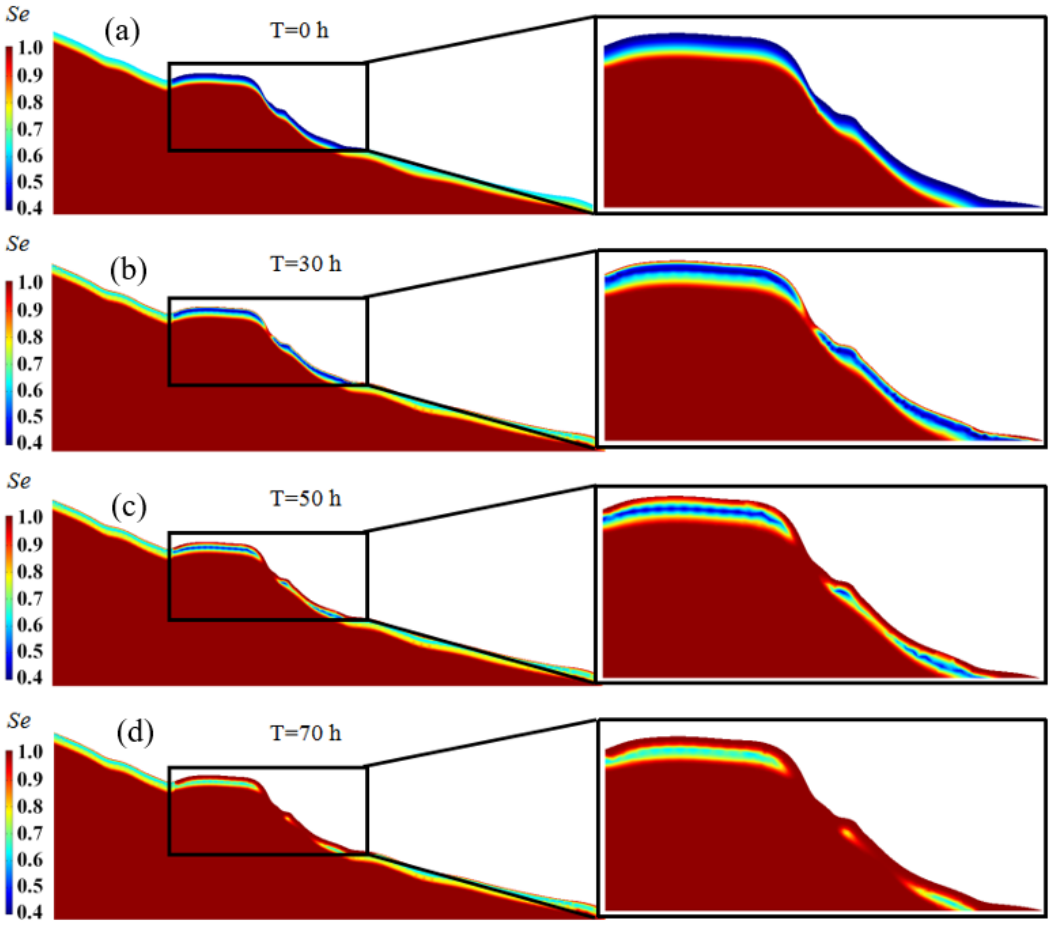

Fig. 11. Distribution of time-dependent effective degree of saturation at Nissho Pass (a) at T=0 h; (b) at T=30 h; (c) at T=50 h; (d) at T=70 h.

Fig. 12 shows the distribution of effective plastic strain (*EPS*) and slope failure shape with large deformation at 15 s in the landslide simulation. A new MPM analysis has been run for each time with different matric suction and local shear strength outputted from FEM analysis. During the MPM analysis, it is assumed that the matric suction and local shear strength for each point keep constant. The above assumption can be considered reasonable since the calculation of MPM is completed in only 15 seconds, which is a very short time so the change of matric suction and local shear strength is neglectable. From Fig. 12. it is recognized that the slope is stable before T=40 h due to a large size unsaturated zone lies above the saturated zone (see Fig. 11). Though high matric suction causes a high

local shear strength of the embankment soil, with the infiltration of rainwater, the matric suction gradually decreases, causing a continuous decrease in local shear strength of the embankment (see Fig. 10). Finally, the slope failure occurred at approximately 40 h (the highway was closed at the same time as shown in Fig. 10) and reached its ultimate shape between 40 h and 50 h (slope failure was complete). Therefore, this simulation has also shown the effectiveness of the proposed hybrid coupled hydro-mechanical framework (FEM-MPM hybrid coupled model) to reproduce and/or predict the rainfall/runoff induced slope failure in unsaturated soil, although the simulated slip surface is shallower compared with the actual one as shown in Fig. 12. The main reason could be that after the occurrence of the landslide, the development of the slip surface caused by the erosion of the newly exposed ground surface by the surface water has not been considered. This needs to be further investigated by considering the continuous erosion of runoff in the proposed FEM-MPM hybrid coupled model, which is one of the limitations of this study currently.

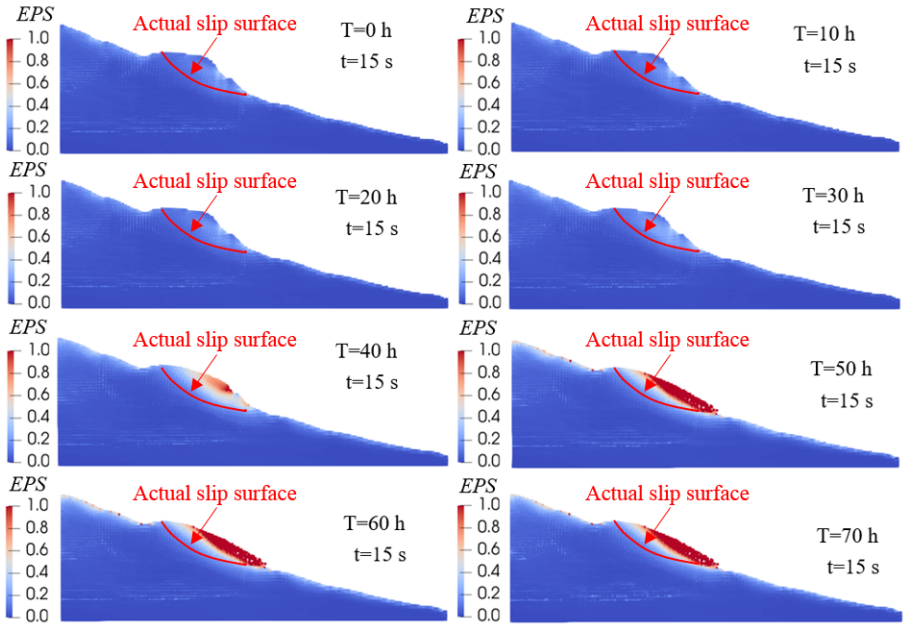

Fig. 12. Distribution of effective plastic strain and slope failure shape with large deformations at Nissho Pass.

6. Discussions and conclusions

This paper proposes a local shear strength method for determining the variable local shear strength corresponding to the variable matric suction for each soil material point within a small catchment-scale unsaturated slope. The local shear strength method built a relationship between the variable local shear strength and the variable matric suction of each soil material point during rainfall/runoff infiltration by shifting the M-C failure envelope.

A hybrid coupled hydro-mechanical framework is proposed based on the local shear strength method to solve rainfall/runoff induced landslide runout in unsaturated slopes. Based on the hybrid coupled hydro-mechanical framework, a FEM-MPM hybrid coupled model is established. The landslide analysis results suggest that the slope stable/unstable state simulated by the FEM-MPM hybrid coupled model has a good consistency with the slip surface simulated by the limit-equilibrium method and shear strength reduction technique. It is proved to be also reliable to simulate the actual slope failure process to determine the occurrence time and location. Therefore, the proposed FEM-MPM hybrid coupled model is proved to be applicable for simulating rainfall/runoff-induced unsaturated soil landslide runout and has the potential to understand the location of landslide initiation and the morphological evolution.

These findings indicate that the local shear strength method and hybrid coupled hydro-mechanical framework proposed in this study provide a feasible way to simulate rainfall/runoff-induced landslide runout in unsaturated soil slopes. It is of great significance to evaluate the landslides movement distance and reasonably recommend the installation of barrier structures to protect the lives and properties of residents living downslope. However, the internal

moisture changes and the dynamic support provided by the runoff during the movement of the landslide are not considered in this study. These should be considered in the future assignments of this study.

Acknowledgments

The authors give sincere thanks to Prof. Zhang Xiong at Tsinghua University for open source their MPM3D code. Since the main works of this study were finished in Hokkaido University, the authors gratefully acknowledge the support of Hokkaido University and Hokkaido Government.

Data Availability

Weather station data used in this research can be downloaded from Japan Meteorological Agency (http://www.data.jma.go.jp/gmd/risk/obsdl/index.php) and terrain information can be got from Geospatial Information Authority of Japan (https://www.gsi.go.jp/top.html).

Declarations

Funding

This research was supported in part by Grant-in-Aids for Scientific Reseach (A) (16H02360) from the Japan Society for the Promotion of Science (JSPS) KAKENHI. This research is also supported by the Fundamental Research Funds for the Central Universities (JB2021043).

Competing Interests

The authors have no relevant financial or non-financial interests to disclose.

References

Abe, K., Soga, K., Bandara, S., 2013. Material point Method for coupled hydromechanical problems. Journal of Geotechnical and Geoenvironmental Engineering. 140(3), 04013033.

Acosta, J.L.G., Vardon, P.J., Hicks, M.A., 2021. Study of landslides and soil-structure interaction problems using the implicit material point method. Engineering Geology. 285, 106043.

An, H., Ouyang, C., Zhou, S., 2021. Dynamic process analysis of the Baige landslide by the combination of DEM and long-period seismic waves. Landslides. 18(5), 1625-1639.

Bishop, A.W., 1959. The principle of effective stress, Teknisk Ukeblad, Norwegian Geotechnical Institute. 106(39), 859-863.

COMSOL Multiphysics. version 5.4, COMSOL Inc., Sweden, 2018.

Fredlund, D.G., Morgenstern, N.R., Widger, R.A., 1978. The shear strength of unsaturated soils. Canadian geotechnical journal. 15, 313-321.

GeoStudio International. GEOSLOPE, Calgary, Alberta, Canada, 2007.

Iverson, R.M., George, D.L., Allstadt, K., et al., 2015. Landslide mobility and hazards: implications of the 2014 Oso disaster. Earth and Planetary Science Letters. 412, 197-208.

Lei, X., He, S., Abed, A., Chen, X., Yang, Z., Wu, Y., 2021. A generalized interpolation material point method for modelling coupled thermo-hydro-mechanical problems. Computer Methods in Applied Mechanics and Engineering. 386, 114080.

Li, X., Yan, Q., Zhao, S., Luo, Y., Wu, Y., Wang, D., 2020. Investigation of influence of baffles on landslide debris mobility by 3D material point method. Landslides. 17, 1129–1143.

447 Liang, D., Zhao, X., Soga, K., 2020. Simulation of overtopping and seepage induced dike failure
448 using two-point MPM. Soils and Foundations. 60(4), 978-988.
449 Müller, A., Vargas, E.A., 2019. Correction to: Stability analysis of a slope under impact of a rock
450 block using the generalized interpolation material point method (GIMP). Landslides. 16, 1063.
451 Ouyang, C., Zhou, K., Xu, Q., et al., 2017. Dynamic analysis and numerical modeling of the 2015
452 catastrophic landslide of the construction waste landfill at Guangming, Shenzhen, China.
453 Landslides. 14(2), 705-718.
454 Ouyang, C., An, H., Zhou, S., et al., 2019. Insights from the failure and dynamic characteristics of two
455 sequential landslides at Baige village along the Jinsha River, China. Landslides. 16(7),
456 1397-1414.
457 Paerl, H.W., Hall, N.S., Hounshell, A.G., et al., 2020. Recent increases of rainfall and flooding from
458 tropical cyclones (TCs) in North Carolina (USA): Implications for organic matter and nutrient
459 cycling in coastal watersheds. Biogeochemistry. 150(2), 197-216.
460 Peng, X., Yu, P., Chen, G., Xia, M., Zhang, Y., 2020. Development of a coupled DDA-SPH method
461 and its application to dynamic simulation of landslides involving solid-fluid interaction. Rock
462 Mechanics and Rock Engineering. 53(1), 113-131.
463 Richards, L.A., 1951. Capillary conduction of liquids through porous mediums. Physics. 1(5),
464 318-333.
465 Sato, A., Hayashi, T., Hayashi, H., Yamaki, M., 2017. On the geotechnical properties of decomposed
466 granite soil in Hokkaido. 57th Technical Report of Hokkaido Branch of Japanese Geotechnical
467 Society. 145-148. (in Japanese)

Shi, G.H., Discontinuous Deformation Analysis A New Numerical Model for the Static and Dynamics of Block Systems. Ph.D. Dissertation, Dept. of Civil Engineering, 1989.

Soga, K., Alonso, E., Yerro, A., Kumar, K., Bandara, S., 2016. Trends in large-deformation analysis of landslide mass movements with particular emphasis on the material point method. Géotechnique. 66 (3), 248-273.

SoilVision. version, 4.23. SoilVision Systems Ltd. Saskatoon, Saskatchewan, Canada, 2018.

Sulsky, D., Chen, Z., Schreyer, H.L., 1994. A particle method for history-dependent materials. Computer Methods in Applied Mechanics and Engineering. 118(1-2), 179-196.

Sun, F., Wang, G., Zhang, L., Wang, R., Cao, T., Ouyang, X., 2021. Material point method for the propagation of multiple branched cracks based on classical fracture mechanics. Computer Methods in Applied Mechanics and Engineering. 386, 114116.

Sun, Y., Yang, J., Song, E., 2015. Runout analysis of landslides using material point method. Iop Conference Series: Earth and Environmental Science. IOP Publishing. 26(1), 012014.

van Genuchten, M. Th., 1980. A closed-form equation for predicting the hydraulic conductivity of unsaturated soils. Soil Science Society of America Journal. 44(5), 892-898.

Vanapalli, S.K., Fredlund, D.G., Pufahl, D.E., Clifton, A.W., 1996. Model for the prediction of shear strength with respect to soil suction. Canadian geotechnical journal. 33(3), 379-392.

Wei, K., Ouyang, C., Duan, H., Li, Y., Chen, M., Ma, J., An, H., Zhou, S., 2020. Reflections on the Catastrophic 2020 Yangtze River Basin Flooding in Southern China. The Innovation. 1(2), 100038.

Weill, S., Mouche, E., Patin, J., 2009. A generalized Richards equation for surface/subsurface flow modelling. Journal of Hydrology. 366(1-4), 9-20.

Woo, S.I., Rodrigo, S., 2018. Simulation of penetration of a foundation element in Tresca soil using the generalized interpolation material point method (GIMP). Computers and Geotechnics. 94, 106-117.

Ying, C., Zhang, K., Wang, Z.N., Siddiqua, S., Makeen, G.M.H., and Wang, L., 2021. Analysis of the run-out processes of the Xinlu Village landslide using the generalized interpolation material point method. Landslides. 18, 1519-1529.

Zhu, Y., Ishikawa, T., Subramanian, S.S., Luo, B., 2020. Simultaneous analysis of slope instabilities on a small catchment-scale using coupled surface and subsurface flows. Engineering Geology. 275, 105750.